Percolation with a periodic boundary condition: The effect of system size for crystallization in molecular dynamics

Makoto S. Watanabe
Faculty of Liberal Arts, Hosei University, Fujimi, Chiyoda-ku, Tokyo 102, Japan
(Received 20 September 1994)

The effect of a periodic boundary condition (PBC) is examined for the percolation process in a square and in simple cubic lattices by means of a Monte Carlo simulation. The universality of the critical exponent for correlation length is valid even for the systems with PBC. The threshold p_c for PBC coincides with the threshold for a free boundary condition in the site percolation of these lattices. We examine the effect of PBC for crystallization processes observed in the molecular dynamics simulation.

PACS number(s): 05.70.Fh, 64.60.Cn

I. INTRODUCTION

Percolation theory has been well known to be applied to many problems in various field of investigations [1]. One of the basic themes in the theory has been to determine the accurate values of thresholds for various lattices. In a practical approach, Monte Carlo (MC) simulation has been well known to be a useful method in estimating their values [1–4]. The thresholds p_c have been derived from extrapolation of the effective thresholds $p(L)$ for the systems with finite spanning size L as $L \to \infty$, i.e., $p_c = p(\infty)$ [1,2].

In usual MC simulations, the shape of the systems has been chosen to be square in the case of two-dimensional (2D) lattices and to be cubic in the case of 3D lattices. The edges of these systems have been treated as a free boundary condition (FBC). Landau [5] has found the influence of a FBC has appeared in the Ising square lattices: the effect of finite size has been greater for an FBC than for a periodic boundary condition [6,7] (PBC).

By means of the MC simulations, Hoshen, Kopelman, and Monberg have found the values of the effective thresholds $p(L)$ with a PBC have been almost equal to the values with an FBC for the site process of the square lattice [8]. Heermann and Stauffer have clarified that the deviations of $p(L)$ from p_c have been larger for a PBC than for an FBC in bond processes of the square lattice [9]. Recently, Ziff has pointed out that obtaining more precise values of $p(L)$ for an FBC than for a PBC is unusual [10]. The origin of the discrepancy, however, has not been clarified yet.

When we examine the values of the thresholds p_c, we extrapolate the effective thresholds $p(L)$ as $L \to \infty$. This is based on the scaling rule $p(L) \propto L^{-1/\nu}$, where ν is a critical exponent for correlation length [1,11,12]. The exponent ν is known to be a dimensional invariant which depends only on the dimensions of lattices. The value of the exponent ν has been found to be $\nu = \frac{4}{3}$ for all lattices in 2D and $\nu = \frac{9}{10}$ in 3D [1,4]. This shows the universality. It has not been clarified, however, whether or not the universality is valid even for the systems with a PBC. In this paper the effect of boundary conditions in the percolation process is examined by use of the MC simulation. The site process has been simulated for the square lattice and for the simple cubic lattice.

From the other point of view, the influence of a PBC has been reported to appear in the crystallization process of supercooled liquids simulated with the molecular dynamics (MD) method [13–15]. The time of onset of catastrophic growth has depended on the system size: the time has increased with increasing size [14]. The origin, however, has not been clarified for the increment of the time. In this paper we apply the scaling rule in percolation theory in order to study the effect of system size in the MD simulation.

In Sec. II we will examine the influence of a PBC for the effective thresholds. The statistical analysis for the square lattice will be presented in Sec. III and for the simple cubic lattice in Sec. IV. In Sec. V, the effect of a PBC will be examined for the crystallization process simulated with the MD method. Discussion will be given in Sec. VI.

II. EFFECTIVE THRESHOLDS AND A PBC

First we have constructed an array of vacant sites on the lattice points of the square lattice in 2D. Their total number N has been $N = L \times L$, where L is the number of the sites on a side of the system. In the array of the vacant sites, an occupied site has been determined at random in the system. Then the number of the occupied sites in the system has been increased at random. Here the cluster structure has been analyzed with the Hoshen-Kopelman algorithm [16] from the occupied sites. The cluster has been defined as a group of sites connected by nearest-neighbor bonds. The increment procedure for the occupied sites has been repeated until the percolation cluster has first appeared through the system. Here the percolation cluster has been defined as the cluster which spans the square cell either horizontally or vertically. This definition corresponds to rule R_0 in Ref. [11].

Here let us see the configuration of the occupied sites when the percolation cluster has first appeared on the lattice. Figure 1(a) shows one of the samples for $L = 100$ under an FBC. The sites are shown as small-filled

squares in a square cell in this figure. The sites, the number of which is $N_s = 5809$ for this sample, scatter widely in the cell. There are isolated sites and connected ones in it. Figure 1(b) shows the shape of the percolation cluster in the cell for the same sample as Fig. 1(a): the sites shown in Fig. 1(b) have been picked out from the occupied sites in Fig. 1(a). The cluster extends from the central part on the left side of the cell to the upper part of the right side of it. This shows horizontal-type percolation under an FBC.

We examine the effect of a PBC for the percolation process in the lattice. Figure 2(a) shows the configuration of the cluster, which is the same cluster as Fig. 1(b), under a PBC: the central cell accompanies eight replicas around it. The replicas have the same cluster as the central cell. No connection of the cluster appears on the left side on the central cell. No connection also appears on the right side of the central cell: a part of the cluster just on the left side in the central cell does not connect with

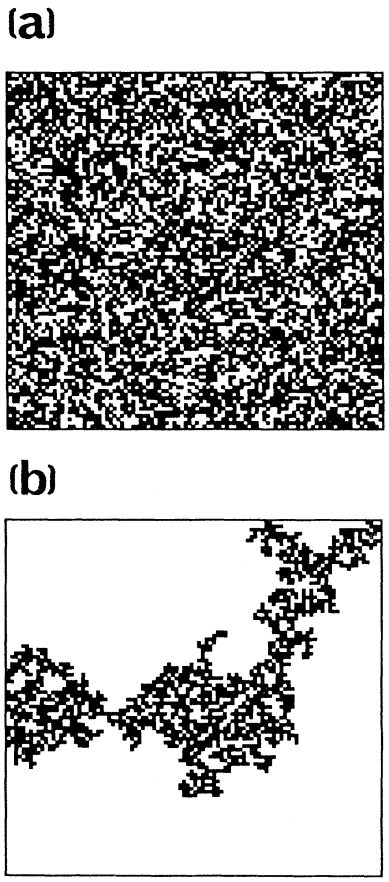

FIG. 1. (a) One of the samples for the distribution of all the occupied sites on the square lattice with an FBC. Their number is $N_s = 5809$ which gives the first appearance of the percolation cluster in the cell. The length of a side on the square cell is $L = 100$. (b) Shape of the percolation cluster in the cell. The sites in (b), which belong to the cluster, are picked out from the sites in (a).

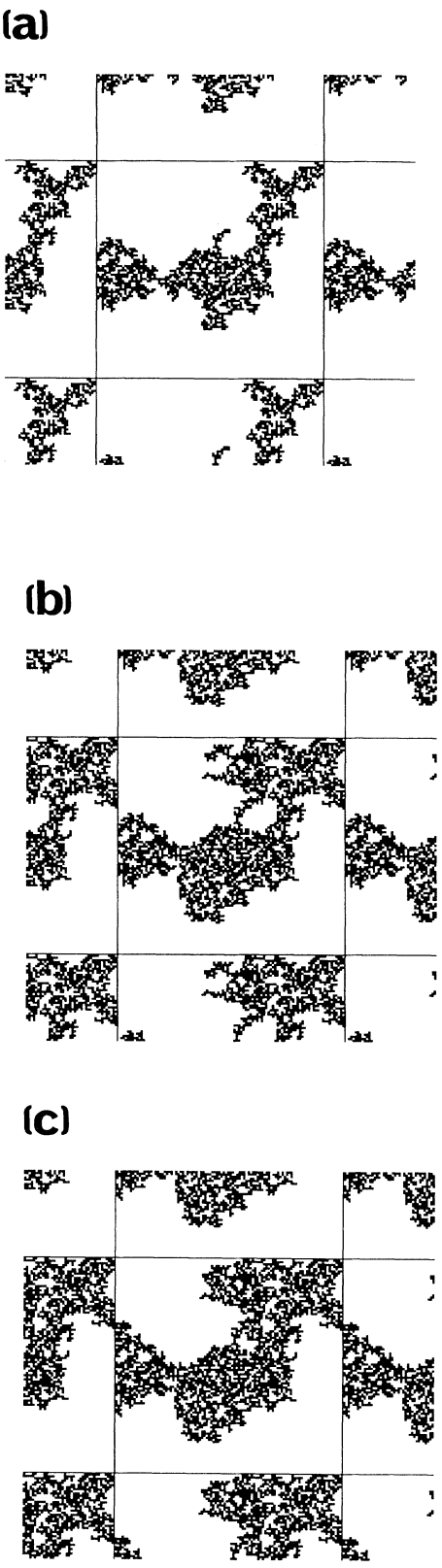

FIG. 2. Development of the shape of the largest cluster on the square lattice with a PBC. The length of a side on the central square cell is $L = 100$. The total numbers of the occupied sites are (a) $N_s = 5809$, (b) $N_s = 6040$, and (c) $N_s = 6268$.

the opposite part of it just on the right side of the left replica. Although the percolation under an FBC has appeared for the sample in Fig. 1(b), it disappears under a PBC as shown in Fig. 2(a).

Here we have increased the number of occupied sites at random and examined the development of the shape of this cluster. Figure 2(b) shows the cluster with a PBC for the number $N_s=6040$ of the sites. Although the shape of the cluster changes within the cell, no connection appears on any side of the cell in this figure. This relation has been valid up to the number $N_s=6267$. Figure 2(c) shows the cluster for the number $N_s=6268$. This number has given the first appearance of the connection cluster through the sides of the cell: a part of the cluster just on the left side of the central cell connects with a part of it just on the right side of the left replica. This shows the percolation appears under a PBC. Figures 2(a)–2(c) suggest the percolation requires larger numbers of occupied sites for a PBC than for an FBC. This shows the effective thresholds are greater for a PBC than for an FBC in the percolation process.

III. THRESHOLD ON THE SQUARE LATTICE

In this section we clarify the relation between the effective thresholds and the system size L for the square lattice by means of the MC simulation. First we have simulated the percolation process with changing the system size as $L=20$, 30, 40, 50, 60, and 100 for the lattice. We have examined the number N_s of occupied sits for the first appearance of the percolation cluster for each L. The number N_s has been averaged with varying simulation samples, i.e., varying the random-number seed, for thousands of times for each L until the average value has converged. Then we have converted it into the fraction $p(L)=N_s/L^2$ which corresponds to the effective threshold for the size L in the system. The results are summarized in Table I, where the first column shows the size L, the second the average fraction $p^{\mathrm{FBC}}(L)$ for an FBC, and the third $p^{\mathrm{PBC}}(L)$ for a PBC. The fractions $p^{\mathrm{FBC}}(L)$ and $p^{\mathrm{PBC}}(L)$ correspond to the effective thresholds with an FBC and with a PBC, respectively. The fractions $p^{\mathrm{FBC}}(L)$ increase with increasing L as shown in Table I. The fractions $p^{\mathrm{PBC}}(L)$ increase with increasing L. The fourth column in Table I shows the absolute values $\Delta p=|p^{\mathrm{FBC}}(L)-p^{\mathrm{PBC}}(L)|$ of the differences between $p^{\mathrm{FBC}}(L)$ and $p^{\mathrm{PBC}}(L)$. The differences decrease with increasing L.

We examine the standard deviations of $p^{\mathrm{FBC}}(L)$ and $p^{\mathrm{PBC}}(L)$ for each L. The fifth column in Table I shows the deviations $\sigma_{\mathrm{std}}^{\mathrm{FBC}}$ for $p^{\mathrm{FBC}}(L)$ and the sixth shows $\sigma_{\mathrm{std}}^{\mathrm{PBC}}$ for $p^{\mathrm{PBC}}(L)$. The deviations $\sigma_{\mathrm{std}}^{\mathrm{FBC}}$ decrease with increasing L. The deviations $\sigma_{\mathrm{std}}^{\mathrm{PBC}}$ have almost the same values as $\sigma_{\mathrm{std}}^{\mathrm{FBC}}$ for each L: the $\sigma_{\mathrm{std}}^{\mathrm{PBC}}$ also decrease with increasing L.

Here we see, in more detail, the differences Δp between the average fractions $p^{\mathrm{FBC}}(L)$ and $p^{\mathrm{PBC}}(L)$ in Table I. The difference Δp for $L=20$ is 0.016 57 which is smaller than $\sigma_{\mathrm{std}}^{\mathrm{FBC}}=0.042\,96$ and than $\sigma_{\mathrm{std}}^{\mathrm{PBC}}=0.040\,96$. This relation is valid for all L in this table: all the differences Δp are smaller than the $\sigma_{\mathrm{std}}^{\mathrm{FBC}}$ and than the $\sigma_{\mathrm{std}}^{\mathrm{PBC}}$ for each L. The ratios $\sigma_{\mathrm{std}}^{\mathrm{PBC}}/\Delta p$ are shown in the seventh column in the table. The ratios are almost constant between 2.42 and 2.65. This indicates the differences are smaller than the deviations which show the extent of the statistical fluctuations for the effective thresholds in this lattice.

Let us examine the value of the threshold p_c as $L\to\infty$. Here we have used the scaling rule [1]:

$$|p_c-p(L)|\propto L^{-1/\nu}, \tag{1}$$

where p_c is the threshold for a system as $L\to\infty$, $p(L)$ the effective thresholds for the system with finite size L, and ν the critical exponent for the correlation length. The exponent ν has been known to be $\frac{4}{3}$ for all lattices with an FBC in 2D [1,4]. The relation (1) gives the other formulation [11,12,17]

$$p(L)=p_c+kL^{-1/\nu}, \tag{2}$$

where k is a constant.

The effective thresholds $p^{\mathrm{FBC}}(L)$ and $p^{\mathrm{PBC}}(L)$, which have appeared in Table I, have been plotted against the scaled size $L_s=L^{-1/\nu}$ with $\nu=\frac{4}{3}$. Figure 3 shows the results. Filled squares are for $p^{\mathrm{FBC}}(L)$ and open ones for $p^{\mathrm{PBC}}(L)$. A linear relation appears between $p^{\mathrm{FBC}}(L)$ and $L^{-1/\nu}$: the $p^{\mathrm{FBC}}(L)$ increase linearly with decreasing $L^{-1/\nu}$. The straight line for $p^{\mathrm{FBC}}(L)$ shows the least-square fitting of the values. The line intersects the abscissa at $p=0.5923$ which deviates by only 0.075% from the accurate value 0.592 746 of the threshold [10] for this lattice. The thresholds $p^{\mathrm{PBC}}(L)$ show the same relation as $p^{\mathrm{FBC}}(L)$: the $p^{\mathrm{PBC}}(L)$ increase linearly with decreasing $L^{-1/\nu}$. This shows the universality of the exponent ν is valid even for a PBC. The line for $p^{\mathrm{PBC}}(L)$ intersects the abscissa at the same point as the above: the threshold for a PBC coincides with the threshold for an FBC as $L\to\infty$.

Although the differences Δp between $p^{\mathrm{FBC}}(L)$ and $p^{\mathrm{PBC}}(L)$ have been smaller than the standard deviations

TABLE I. The effective thresholds and the standard deviations for the square lattice with an FBC and a PBC.

L	$p^{\mathrm{FBC}}(L)$	$p^{\mathrm{PBC}}(L)$	Δp	$\sigma_{\mathrm{std}}^{\mathrm{FBC}}$	$\sigma_{\mathrm{std}}^{\mathrm{PBC}}$	$\sigma_{\mathrm{std}}^{\mathrm{PBC}}/\Delta p$
20	0.568 81	0.585 38	0.016 57	0.042 96	0.040 96	2.47
30	0.575 00	0.587 57	0.012 57	0.033 90	0.031 73	2.52
40	0.577 76	0.587 79	0.010 03	0.027 49	0.026 60	2.65
50	0.580 30	0.589 03	0.008 73	0.023 69	0.022 22	2.55
60	0.582 18	0.590 32	0.008 14	0.021 01	0.019 69	2.42
100	0.585 34	0.590 94	0.005 60	0.014 28	0.013 66	2.44

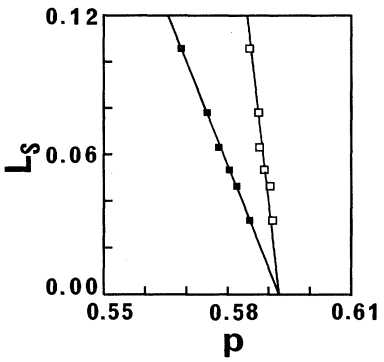

FIG. 3. The effective thresholds against the scaled size $L_s = L^{-1/\nu}$ for the square lattice. The exponent ν is $\frac{4}{3}$ for this system. Filled squares are for $p^{\mathrm{FBC}}(L)$ and open ones for $p^{\mathrm{PBC}}(L)$.

for each L as shown in Table I, the clear relation appears between them as shown in Fig. 3: the effective thresholds are closer to p_c for a PBC than for an FBC in the case of the site process of the square lattice.

IV. THRESHOLD ON THE SIMPLE CUBIC LATTICE

In this section we clarify the relation between the effective thresholds and the system size L for the simple cubic lattice by means of the MC simulation. First we have constructed an array of the vacant sites with the total number $N = L \times L \times L$ in the cubic cell. A percolation process has been simulated with changing the system size as $L = 12, 15, 18, 20$ for this lattice. We have examined the number N_s of occupied sites for the first appearance of the percolation cluster. The number N_s has been averaged with varying simulation samples. Then we have converted it into the fraction $p(L) = N_s / L^3$ which corresponds to the effective thresholds for each L. The percolation cluster has been defined as the cluster which spans the cubic cell at least in one direction. This condition corresponds to the rule R_0 in Ref. [11] in the case of 3D lattices. The results are shown in Table II, where the first column shows the size L, the second the average fraction $p^{\mathrm{FBC}}(L)$ for an FBC, and the third $p^{\mathrm{PBC}}(L)$ for a PBC. The fractions $p^{\mathrm{FBC}}(L)$ increase with increasing L as shown in Table II. The fractions $p^{\mathrm{PBC}}(L)$ decrease with increasing L. The fourth column in Table II shows the absolute values $\Delta p = |p^{\mathrm{FBC}}(L) - p^{\mathrm{PBC}}(L)|$ of the differences between $p^{\mathrm{FBC}}(L)$ and $p^{\mathrm{PBC}}(L)$ for each L. The differences decrease with increasing L.

We examine the standard deviations of $p^{\mathrm{FBC}}(L)$ and $p^{\mathrm{PBC}}(L)$. The fifth column in Table II shows the deviations $\sigma_{\mathrm{std}}^{\mathrm{FBC}}$ for $p^{\mathrm{FBC}}(L)$ and the sixth shows $\sigma_{\mathrm{std}}^{\mathrm{PBC}}$ for $p^{\mathrm{PBC}}(L)$. The deviations $\sigma_{\mathrm{std}}^{\mathrm{FBC}}$ decrease with increasing L. The deviations $\sigma_{\mathrm{std}}^{\mathrm{PBC}}$ have almost the same values as $\sigma_{\mathrm{std}}^{\mathrm{FBC}}$ for each L: the deviations $\sigma_{\mathrm{std}}^{\mathrm{PBC}}$ decrease with increasing L.

Here we see, in more detail, the differences Δp between the average fractions $p^{\mathrm{FBC}}(L)$ and $p^{\mathrm{PBC}}(L)$ in Table II. The difference Δp for $L = 12$ is 0.023 26 which is smaller than $\sigma_{\mathrm{std}}^{\mathrm{FBC}} = 0.027\,84$ and than $\sigma_{\mathrm{std}}^{\mathrm{PBC}} = 0.025\,30$. This relation is valid for all L in this table: all the differences Δp are smaller than the $\sigma_{\mathrm{std}}^{\mathrm{FBC}}$ and than the $\sigma_{\mathrm{std}}^{\mathrm{PBC}}$ for each L. The ratios $\sigma_{\mathrm{std}}^{\mathrm{PBC}}/\Delta p$ are shown in the seventh column in the table. The ratios are almost constant between 1.02 and 1.09. This indicates the differences are smaller than the deviations which show the extent of the statistical fluctuations for the effective thresholds in this lattice.

In order to examine the value of p_c as $L \to \infty$, we have used the scaling rule (2). The exponent ν in (2) has been found to be $\frac{9}{10}$ for all lattices with an FBC in 3D [1,4]. The effective thresholds $p^{\mathrm{FBC}}(L)$ and $p^{\mathrm{PBC}}(L)$, which have appeared in Table II, have been plotted against the scaled size $L_s = L^{-1/\nu}$ with $\nu = \frac{9}{10}$. Figure 4 shows the results. Filled squares are for $p^{\mathrm{FBC}}(L)$ and open ones for $p^{\mathrm{PBC}}(L)$. The values $p^{\mathrm{FBC}}(L)$ increase linearly with decreasing $L^{-1/\nu}$. The straight line for $p^{\mathrm{FBC}}(L)$ shows the least-square fitting of the values. The line for $p^{\mathrm{FBC}}(L)$ intersects the abscissa at $p = 0.3115$ which deviates by only 0.064% from the value 0.3117 of the threshold [1,4] for this lattice. A linear relation appears between $p^{\mathrm{PBC}}(L)$ and $L^{-1/\nu}$: the $p^{\mathrm{PBC}}(L)$ decrease linearly with decreasing $L^{-1/\nu}$. This indicates the universarity of the exponent ν is valid even for a PBC. The line for $p^{\mathrm{PBC}}(L)$ intersects the abscissa at the same point as the above: the thresholds p_c for a PBC coincides with the threshold for an FBC as $L \to \infty$.

Although the differences Δp between $p^{\mathrm{FBC}}(L)$ and $p^{\mathrm{PBC}}(L)$ have been smaller than the standard deviations for each L as shown in Table II, the clear relation appears between them as shown in Fig. 4: the effective thresholds are closer to p_c for an FBC than for a PBC in the case of the site process of the simple cubic lattice. This result differs from the result for the square lattice: accuracy of $p(L)$ varies from system to system in the process.

V. CRYSTALLIZATION AND SYSTEM SIZE

Influence of system size has been reported to appear in the crystallization process from the liquid state by means

TABLE II. The effective thresholds and the standard deviations for the simple cubic lattice with an FBC and a PBC.

L	$p^{\mathrm{FBC}}(L)$	$p^{\mathrm{PBC}}(L)$	Δp	$\sigma_{\mathrm{std}}^{\mathrm{FBC}}$	$\sigma_{\mathrm{std}}^{\mathrm{PBC}}$	$\sigma_{\mathrm{std}}^{\mathrm{PBC}}/\Delta p$
12	0.306 13	0.329 39	0.023 26	0.027 84	0.025 30	1.09
15	0.307 66	0.326 16	0.018 50	0.020 96	0.019 46	1.05
18	0.308 15	0.324 11	0.015 96	0.017 92	0.016 33	1.02
20	0.308 41	0.322 33	0.013 92	0.016 27	0.014 43	1.04

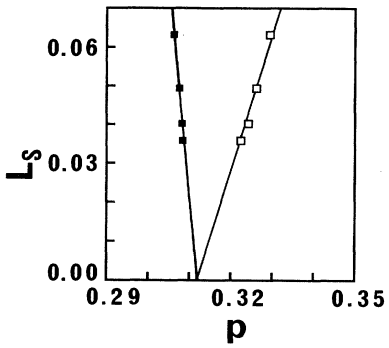

FIG. 4. The effective thresholds against the scaled size $L_s = L^{-1/\nu}$ for the simple cubic lattice. The exponent ν is $\frac{9}{10}$ for this system. Filled squares are for $p^{\mathrm{FBC}}(L)$ and open ones for $p^{\mathrm{PBC}}(L)$.

of the MD simulation [13–15]. Tanemura *et al.* have simulated homogeneous nucleation and growth processes in the supercooled liquid of the soft-core system [13]. They have found a PBC has influenced the shape of the nucleus formed in the liquid with the simulation: the nucleus has developed with time anisotropically in the liquid [13]. Honeycutt and Andersen have examined the time to catastrophic growth of the crystal in the supercooled liquid of the Lennard-Jones system [14,15]. They have found the time has depended on the total number N of atoms in the simulation: the time increased with increasing system size N [14]. Figure 5, which has been presented in Ref. [14], shows the time as a function of the number N. Filled squares are for the average time for each N. The time increases with increasing N and seems to saturate at time between $t=100$ and $t=120$ as $N \rightarrow \infty$. They have found the number of the atoms in the critical nucleus for growth has depended on the system size: their number has increased with increasing system size [15]. The above results may imply the classical nucleation theory is inefficient in describing the crystallization process observed in the MD simulation with a PBC: the theory assumes the shape of the nucleus is spherical and its size is constant for a specified material.

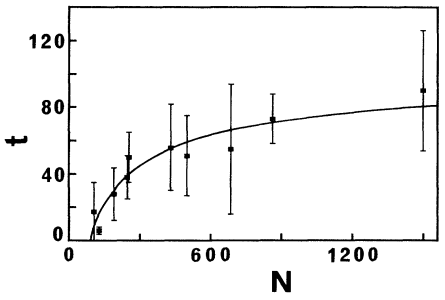

FIG. 5. The time to catastrophic growth of the crystal as a function of the system size N in the MD simulation. Filled squares are for the average time which have been presented in Ref. [14]. The unit of the ordinate is $\tau=(m\sigma^2/\varepsilon)^{1/2}$, where m is the mass of an atom, ε is the Lennard-Jones attraction parameter, and σ corresponds to the distance at the first zero of the potential. A curve shows the least-square fitting of formula (6).

Here let us interpret the relation in Fig. 5 in the framework of the percolation theory. First we consider solidlike atoms in supercooled liquid as occupied sites in the percolation system. Then we increase the number of occupied sites, as the increment of the number of atoms with time, at random in the MC cell. This shows time in the MD systems corresponds to the fraction p of the number of the occupied sites to the total number of the sites in the MC systems. Here we regard the appearance of the percolation cluster in the MC cell with a PBC as the formation of the critical nucleus in the MD cell with a PBC. Since the size of the "nucleus" in the above model is infinite under a PBC, such a nucleus can grow certainly in liquids and never vanishes. The formation of the critical nucleus means the onset of crystal growth in the system. Thus the effective thresholds correspond to the time of onset of the growth in the MD simulation. Jouhier *et al.* have analyzed solidification processes (sol-gel transition) of a polymer by the use of the same model as the above [18]. In this study, they have considered that the relation between the fraction p and time is linear: solidification time has been regarded as the percolation threshold [18].

Let us apply the above model in order to clarify the relation between the time and the system size. First we rewrite formula (2) as

$$t(L)=t(\infty)+kL^{-1/\nu}, \tag{3}$$

with the following relation:

$$t(L) \propto p(L), \tag{4}$$

where $t(L)$ is the time of onset of catastrophic growth for system size L in the MD simulation. Here the size L is $L=N^{1/3}$, where N corresponds to the total number of atoms in the MD cell. Formula (3) is transformed into

$$t(L)=t(\infty)+kN^{-1/3\nu}. \tag{5}$$

In Sec. IV, the value of ν has been found to be $\nu=\frac{9}{10}$ for the percolation system with a PBC in the case of a 3D lattice. This gives

$$t(L)=t(\infty)+kN^{-10/27}. \tag{6}$$

Here we examine whether or not formula (6) is valid for the relation between the time to the growth of the crystal and the system size N as shown in Fig. 5. We have obtained the values of $t(\infty)$ and k in (6) by use of the least-square fitting of the average time in Fig. 5. The values have been found to be $t(\infty)=124.3$ and $k=-657.6$. A curve in this figure shows the result with these values. The curve is found to be suitable in approximating the relation between the time and the system size N. This shows formula (6) is valid in describing the effect of the system size for the time of onset of catastrophic growth of the crystal observed in the MD simulation with a PBC.

VI. DISCUSSION

We have found the standard deviations in Tables I and II have depended on the system size L for the square and the simple cubic lattices: the values of the deviations have decreased with increasing L. Here we see the deviation as $L \to \infty$. Figure 6 shows the deviations of $p^{\mathrm{FBC}}(L)$ and $p^{\mathrm{PBC}}(L)$ for the square lattice. Filled squares are for $p^{\mathrm{FBC}}(L)$ and open ones for $p^{\mathrm{PBC}}(L)$. The standard deviations for each L are shown as the error bars around them. Straight lines in this figure show the extrapolation of the deviations. All the lines in Fig. 6 converge on the same point on the abscissa. This indicates the width of the deviation is 0 as $L \to \infty$ not only for an FBC but also for a PBC in the square lattice. Figure 7 shows the deviations of $p^{\mathrm{FBC}}(L)$ and $p^{\mathrm{PBC}}(L)$ for the simple cubic lattice. Filled squares are for $p^{\mathrm{FBC}}(L)$ and open ones for $p^{\mathrm{PBC}}(L)$. The standard deviations for each L are shown as the error bars around them. Straight lines show the extrapolation of the deviations. All the lines in Fig. 7 converge on the same point on the abscissa. This indicates the width of the deviations is 0 as $L \to \infty$ not only for an FBC but also for a PBC in the simple cubic lattice.

By means of the percolation model as shown in Sec. V, the effect of system size has been examined for the time of onset of crystal growth in the MD simulation. In this model we have increased the number of occupied sites in the MC cell as increments of the number of solidlike atoms with time in the MD cell. This is found to be valid from the following fact. In the MD simulations, we have observed decrement of pressure [19] and volume [20] of systems with time from onset of annealing prior to the crystallization event. We have found some parameters, which analyze local arrangement of atoms, have changed with time in the simulation from the onset of annealing [20]. The local symmetry parameter $\hat{W}_6$, Volonoi face ratio n_4, and the ratio n_6 have increased with time. On the other hand, the ratio n_5 has decreased with time in the simulation [20]. These changes indicate the number of atoms with local crystal structure has increased with time from the onset of annealing prior to the event. This

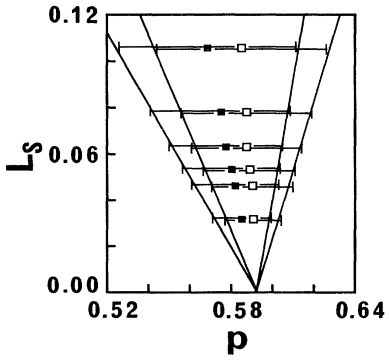

FIG. 6. Standard deviations around the effective thresholds for the square lattice. Filled squares are for $p^{\mathrm{FBC}}(L)$ and open ones for $p^{\mathrm{PBC}}(L)$. The deviations are shown as the error bars around them. Straight lines are the extrapolation of the deviations.

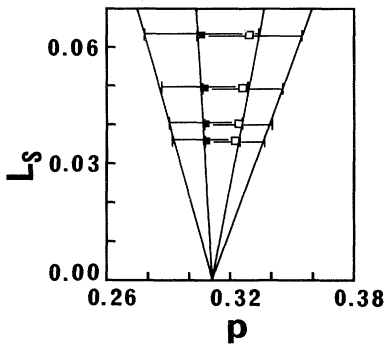

FIG. 7. Standard deviations around the effective thresholds for the simple cubic lattice. Filled squares are for $p^{\mathrm{FBC}}(L)$ and open ones for $p^{\mathrm{PBC}}(L)$. The deviations are shown as the error bars around them. Straight lines are the extrapolation of the deviations.

is the evidence for the increment of the atoms with local crystal structure in annealing simulations with time. This shows the above model, i.e., correspondence between the fraction p and time, is valid in describing the crystallization process observed in the MD simulation.

In this model, we have defined the formation of the critical nucleus in the MD simulation as the appearance of the percolation cluster in the MC simulation. This implies the nucleus formed in the MD simulation should extend through the simulation cell. This definition is found to be valid. Tanemura *et al.* have found the nucleation has proceeded anisotropically with a one-dimensional extension of the nucleus from one side to the other side of the cubic cell with time in the supercooled liquid of the soft-core system by means of the MD simulation [13]. This contradicts the classical nucleation theory which predicts a spherical nucleus in the liquid. Honeycutt and Andersen have examined the shape of nuclei formed in the supercooled liquid of the Lennard-Jones system with the MD simulation [15]. They have used the linear-triplet method for a central atom in order to know whether or not the central atom has local crystal structure around it. The shape of the nucleus formed in the liquid has been anisotropic for the criteria 162° and 165° which are cutoff angles in the linear triplet around an atom. The weaker criterion 159°, however, has not given anisotropic extension of the nucleus, but it has given a spherical extension in the system showing the validity of the classical nucleation theory. This criterion may be adequate for the identification of the nucleus appearing in the liquid. This criterion has allowed the nucleus to extend between the faces through the simulation cell [15]. They have stated that crystal growth begins when the nucleus becomes large enough to feel the influence of its periodic images [14]: the critical nucleus must interact with its images [15]. This indicates the above definition of the critical nucleus, i.e., correspondence between the nucleus in the MD simulation and the percolation cluster in the MC simulation, is suitable.

The influence of the system size has been examined for

the crystallization process with formula (6) in Sec. V. The relation has included the exponent $\nu=\frac{9}{10}$ which has been found from the MC simulation for a percolation system with a PBC in 3D. The exponent has shown the same value for the system with an FBC. This indicates the relation between the time to growth and the system size is the same as Fig. 5 for crystallization processes in the MD simulation with an FBC: formula (6) may be suitable even for the systems with an FBC. It is difficult to examine, however, whether or not the formula is valid even for the systems with an FBC in the MD simulations, since the simulation with an FBC inevitably accompanies the surface effect which comes from the interactions between atoms.

[1] D. Stauffer, *Introduction to Percolation Theory* (Taylor & Francis, London, 1985).
[2] D. Stauffer, Phys. Rep. **54**, 1 (1979).
[3] D. W. Heermann, *Computer Simulation Methods in Theoretical Physics* (Springer-Verlag, Berlin, 1990).
[4] T. Odagaki, *Introduction to Percolation Physics* (Shokabo, Tokyo, 1993) (in Japanese).
[5] D. P. Landau, Phys. Rev. B **13**, 2997 (1976).
[6] N. Metropolis, A. W. Rosenbluth, M. N. Rosenbluth, and A. H. Teller, J. Chem. Phys. **21**, 1087 (1953).
[7] W. W. Wood and F. R. Parker, J. Chem. Phys. **27**, 720 (1957).
[8] J. Hoshen, R. Kopelman, and E. M. Monberg, J. Stat. Phys. **19**, 219 (1978).
[9] D. W. Heermann and D. Stauffer, Z. Phys. B **40**, 133 (1980).
[10] R. M. Ziff, Phys. Rev. Lett. **69**, 2670 (1992).
[11] P. J. Reynolds, H. E. Stanley, and W. Klein, Phys. Rev. B **21**, 1223 (1980).
[12] F. Yonezawa, S. Sakamoto, and M. Hori, Phys. Rev. B **40**, 636 (1989); **40**, 650 (1989).
[13] M. Tanemura, Y. Hiwatari, H. Matsuda, T. Ogawa, N. Ogita, and A. Ueda, Prog. Theor. Phys. **58**, 1079 (1977).
[14] J. D. Honeycutt and H. C. Andersen, Chem. Phys. Lett. **108**, 535 (1984).
[15] J. D. Honeycutt and H. C. Andersen, J. Phys. Chem. **90**, 1585 (1986).
[16] J. Hoshen and R. Kopelman, Phys. Rev. B **14**, 3438 (1976).
[17] P. J. Reynolds, H. E. Stanley, and W. Klein, J. Phys. A **11**, L199 (1978).
[18] B. Jouhier, C. Allain, B. Gauthier-Manuel, and E. Guyon, in *Percolation Structures and Processes,* edited by G. Deutscher, R. Zallen, and J. Adler (Adam Hilger, Bristol, 1983), p. 167.
[19] M. J. Mandell, J. P. McTague, and A. Rahman, J. Chem. Phys. **64**, 3699 (1976).
[20] F. Yonezawa, S. Nosé, and S. Sakamoto, J. Non-Cryst. Solids **97&98**, 373 (1987).